The Additive Cytotoxic Effect of BMS754807 and BMS599626 on the Head and Neck Cancer Proteome

Authors:

Sarah Hall

Mark Jameson, M.D., Ph.D., FACS

Dan Gioeli, Ph.D.

Words: 2236

Number of Figures: 6

Number of Tables: 0

Number of Equations: 1

Number of Supplements: 1

Number of References: 11

Signed Approval _____Date___05/08/2021_____

The Additive Cytotoxic Effect of BMS754807 and BMS599626 on the Head and Neck Cancer Proteome

Sarah P. Hall[a1], Mark Jameson, M.D., Ph.D., FACS[b], Daniel Gioeli, Ph.D.[c]

[a] Fourth Year Biomedical Engineering Undergraduate, University of Virginia
[b] Department of Otolaryngology, University of Virginia
[c] Department of Microbiology, Immunology, and Cancer Biology, University of Virginia
[1] Correspondence: sph8zz@virginia.edu

Abstract

Head and neck cancers are the sixth most common cancer worldwide. Combinatorial targeted therapy has the potential to reduce drug resistance and increase cytotoxicity to cancer cells, including head and neck squamous cell carcinoma (HNSCC). The epidermal growth factor receptor (EGFR) is overexpressed in more than 90% of HNSCCs, and therefore poses as a promising target for chemotherapeutics. However, we previously demonstrated that the insulin-like growth factor 1 receptor (IGF1R) becomes activated as a mechanism for resistance against EGFR inhibition. Thus, an IGF1R inhibitor, BMS754807, and an EGFR inhibitor, BMS599626, were used in combination to combat resistance to EGFR inhibition alone. The combination of BMS754807 and BMS599626 robustly inhibited the grown of HNSCC cell lines in vitro. To examine the mechanism of cytotoxicity, reverse phase protein array (RPPA) data of 145 epitopes in five HNSCC cell lines was analyzed using Python. By calculating log fold changes, running t-tests, performing principal component analysis, and examining cell line gene mutations, we were able to provide a plethora of evidence to support the hypothesis that the combination has a potentiative effect on inhibiting signaling downstream of IGF1R and EGFR. The effects of the individual drugs are amplified, demonstrating that the combination more robustly inhibits the pathways of both receptors. This targeted therapy method is significant because HNSCC patients need safer, less invasive, and more precise treatment options.

Keywords: HNSCC, EGFR, IGF1R, RPPA, resistance

Introduction

Head and neck cancers are the sixth most prevalent cancer type worldwide with a 65% survival rate five year after diagnosis in the United States.[1] Approximately 630,000 patients are diagnosed annually with more than 350,000 deaths each year and these cancers affect roughly 14.97 men and 6.24 women per 100,000.[1,2] These types of cancers can occur in the nose, oral cavity, tongue, tonsils, and the sinuses.[1] Most are squamous cell carcinomas (SCC), which develop in epithelial cells, and are associated with tobacco and alcohol use.[3]

Current treatment methods for head and neck squamous cell carcinoma (HNSCC) include surgery, radiation therapy, and chemotherapy. While some tumors can simply be removed, a major risk for any operation is loss of function in that area, including the inability to talk or the inability to swallow. A common procedure that aims at reducing this risk is the utilization of microvascular free flaps. This technique involves using the patient's own tissue at a secondary location to reconstruct the cancerous area. For example, a surgeon can use the muscles of the forearm to restore function of the tongue. However, any surgical procedure is invasive and creates a risk of infection. Moreover, surgery for HNSCC is often disfiguring and can lead to difficulties breathing, speaking, and swallowing. Also, surgery alone can rarely eradicate the cancer. Typically, patients who have operations are also treated with radiation and/or chemotherapy. Radiation therapy (RT) can be used as a single-modality treatment method for early signs of HNSCC, but typically is used in combination with another therapeutic. While radiation has desirable cytotoxic abilities, this method cannot target cancerous cells specifically, resulting in the death of surrounding cells and patients suffering from additional side effects.[4] There is a prevalence of dysphagia in patients five or more years after being treated with radiotherapy.[5] Lastly, chemotherapy is extremely harmful to the body, and is rarely used independently. While these treatment options can be

effective, a less invasive, more specific, and more permanent method is needed.[4]

Targeted therapy is a newer method of treatment for cancer. The goal of targeted therapy is to inhibit proteins involved in signaling pathways that are activated for survival/migration/invasion.[6]

While single-targeted drugs can initially show success in killing cancer cells, mechanisms of resistance arise. For example, treatment of KRAS-mutant lung cancer with trametinib, a MEK inhibitor that acts via the mitogen-activated protein kinase (MAPK) pathway, results in developed resistance involving fibroblast growth factor receptor 1 (FGFR1). Therefore, trametinib used in combination with an FGFR1 inhibitor was tested to determine efficacy *in vitro* and *in vivo*, and cancer cell death increased.[7] In HNSCC, epidermal growth factor receptor (EGFR) has been shown to play an integral role in cell growth and metastasis and is overexpressed in more than 90% of tumors.[8,9] Previously, our lab generated data to support the connection between insulin-like growth factor 1 receptor (IGF1R) and EGFR, where IGF1R activation is a mechanism for resistance in response to EGFR inhibition. Both of these targets are receptor tyrosine kinases (RTKs): transmembrane proteins that are activated by ligands leading to activation of signal transduction networks.[10] The combination of an EGFR inhibitor (BMS599626) and an IGF1R inhibitor (BMS754807) has an additive effect on HNSCC cytotoxicity. Nine cell lines were tested: Cal27, Fadu, OSC19, SCC9, SCC25, SCC25GR1, SCC61, UNC7, and UNC10. All cell lines showed >55% growth inhibition. This experiment showed evidence to support the hypothesis that crosstalk between IGF1R and EGFR form a mechanism of drug resistance, but this mechanism is prevented when both receptors are inhibited.[9]

We performed computational analysis on reverse phase protein array (RPPA) data. The data contained expression values of 145 epitopes across five cell lines, five time points, and four drugs. The cell lines utilized were Cal27, Fadu, SCC9, SCC25, and OSC19, the time points were 15 minutes, 1 hour, 3 hours, 8 hours, and 24 hours, and the drugs were control/vehicle, BMS599626, BMS754807, and the two inhibitors used in combination. The data was examined using various methods in order to see how the drugs alter the HNSCC proteome. We performed this investigation to determine if new proteins of interest would emerge as targets or if the combination would enhance the effects of the individual drugs. By doing so, we can better understand how and why cells are dying by discovering which protein pathways are being affected. Ultimately, this information is useful to improve targeted therapy for head and neck cancers.

Results

Log fold change

To initially visualize changes in epitope expression, log base 2 fold changes were calculated for each drug (Equation 1).

$$\text{Log FC} = \frac{log_2[drug]}{log_2[control]} - 1 \qquad \text{(Eq. 1)}$$

In Python, a heatmap was generated to display changes in all epitopes across all time points, cell lines, and drugs (Figure 1). Hierarchical clustering was performed in order to find groups of epitopes that behaved similarly in response to the combination. Phosphorylation sites of IGF1R and EGFR as well as downstream epitopes were clustered together, as expected based on the targets of the individual drugs. Treatment with the combination did not result in unique epitope changes, showing evidence to support the hypothesis that the combination leads to further decrease in signaling already effected by the single drugs. Epitopes not targeted by the individual drugs did not have large changes in expression. Overall, the combination shows greater inhibition or amplification of epitope signal compared to each drug individually. In cluster 6, which contains Janus Kinase 2 (Jak2) Y1007 and platelet-derived growth factor receptor (PDGFR) beta Y751, BMS754807 has a larger effect on protein phosphorylation than BMS599626 as these proteins are downstream targets of IGF1R. The combination has a similar effect compared to treatment with BMS754807 alone, showing that the IGF1R inhibitor is driving the effect of the combo for this cluster of epitopes. In cluster 7, which includes EGFR Y1068, EGFR Y1173, and human epidermal growth factor receptor 2 (HER2) Y1248, neither individual drug affects epitope levels as drastically as the combination. This cluster demonstrates the potency of the combination compared to using one drug, which is seen in other clusters as well. When time and/or cell line data was compressed, the epitopes of interest remained the same, demonstrating that the combination robustly impacts the proteome regardless of the cell line or time point being tested. (Supplemental Figure 1)

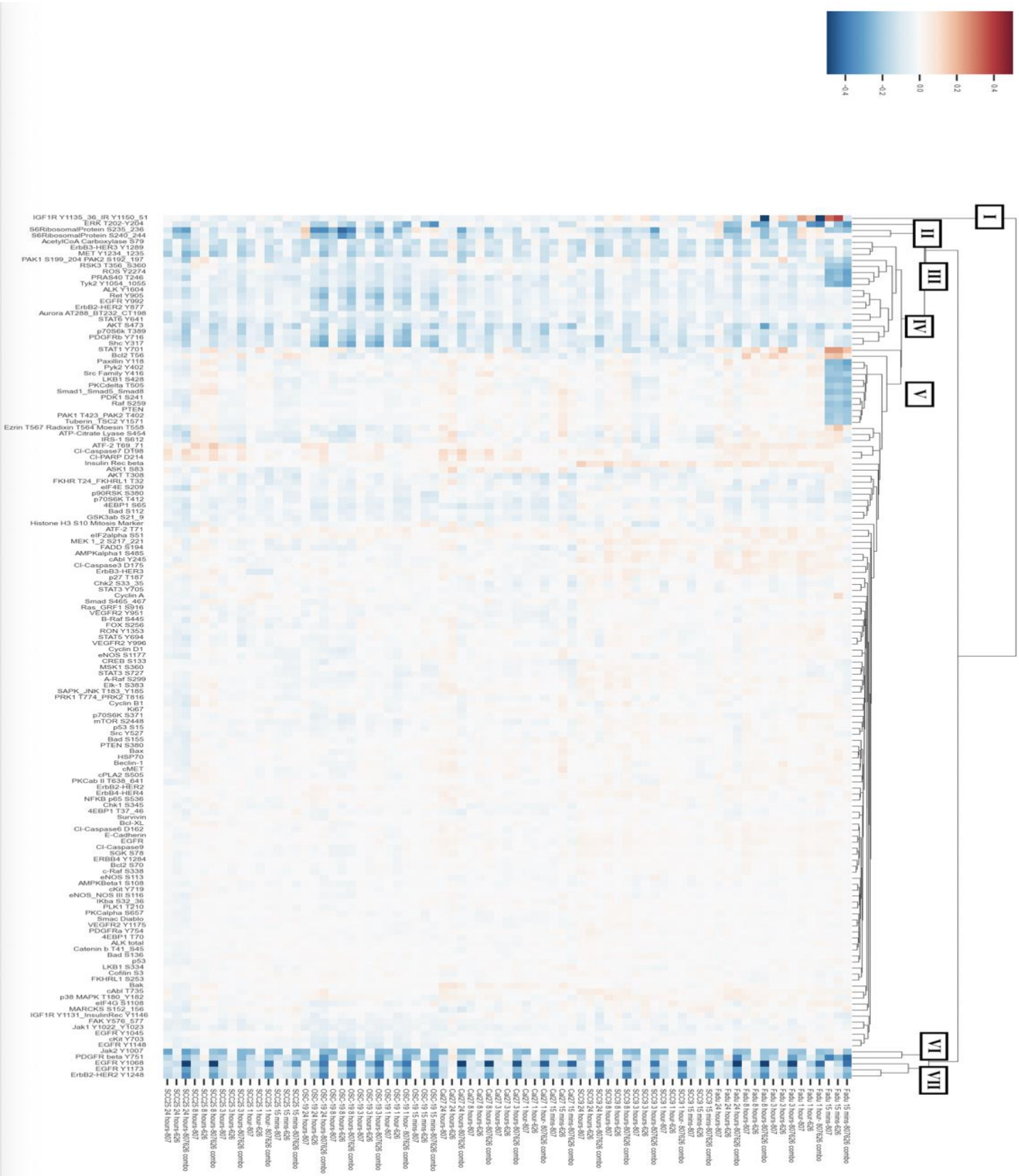

Figure 1: Log FC Heatmap. Heatmap of log fold changes for each drug condition compared to control. Conditions are on the x axis and 145 epitopes are on the y axis. Cell lines used were SCC9, SCC25, Cal27, OSC19, and Fadu and time points were 15 mins, 1 hour, 3 hours, 8 hours, and 24 hours. Red depicts an increase in expression and blue depicts a decrease. Hierarchical clustering revealed seven key clusters of epitopes.

Statistical Analysis

In order to determine if epitope signal changes were significant, t-tests were performed to compare each condition. Benjamini-Hochberg False Discovery Rate (FDR) adjusted p-values were generated and a significance level of 0.05 was used. In Figure 2, all comparisons are displayed, with p-values below 0.05 being highlighted. Proteins present in the clusters from log FC calculations were also statistically significant. Therefore, the results of these tests supported the notion that the combination significantly changes expression of epitopes that are downstream targets of EGFR and IGF1R. Importantly, comparisons between the individual drugs and the control group were rarely significant, showing that using a single drug is not effective in altering protein expression. However, comparing the combination to each drug alone or to control showed significance for many epitopes which illustrates the potency of using these drugs together to treat HNSCC cells.

Principal Component Analysis

To reduce noise in the data and uncover overall trends, principal component analysis was performed. Principal components (PCs) were generated, which serve as new variables that are linear combinations of the original variables (cell lines, time points, and drugs). The first PC contains the most variance in the data, followed by the second PC, third PC, etc. PC plots were created in Python and color-coded based on which variable each point represented. Data points were clustered precisely based on cell lines, revealing that cell lines dominated variance in the data. (Figure 3). Following this discovery, PCA was performed on data from each cell line and color-coded based on time point and drug (Figure 4). Due to clustering of data points based on treatment, we determined that drug treatment was the second most influential variable. Based on these PC plots, we were able to see how each drug impacted the different cell lines. For example, in SCC9s the BMS754807 data points align with those for the combination, showing that the IGF1R inhibitor is driving the effect of the combination in this cell line. Conversely, in Cal27s the combo data points do not cluster with those for either individual drug, demonstrating that the combination has a unique effect on this cell line that is not driven by the effects of one drug. Coloring by time point showed no obvious trends, meaning that changes in protein expression were not determined by time.

To discover which epitopes varied the most in each PC, loadings for all 145 epitopes were calculated and ranked. Loadings values display the weight that each epitope has on overall PC variance. The top 15 epitopes for each PC in each cell line were plotted (Figure 5), with greater distance from the origin demonstrating a larger weight. The epitopes that were present in the log FC clusters and that showed statistical significance from t-tests had the largest loadings across all cell lines, further illustrating that the primary effect of the combination is to enhance inhibition of signaling observed with the single drugs.

Cell Line Gene Mutations

Cell line gene mutations were examined in order to visualize heterogeneity in the cell lines used in the RPPA data and determine if these mutations were driving response to the drugs seen in the PCAs. The cBioPortal for cancer genomics was used to gather a list of mutated genes and their frequencies across 515 HNSCC tumors. The Cancer Cell Line Encyclopedia was then used to identify mutations in the cell lines tested in the RPPA data. The lists of mutations for each cell line were compared to the general list of HNSCC mutations and common genes were identified. (Figure 6) The lack of uniformity across cell lines furthers the point found from PCA that cell heterogeneity within a tumor determines behavior in response to treatment more than other variables.

Discussion

Current methods for treating HNSCC are extremely invasive and generally result in loss of vital functions such as swallowing or speech. Targeted therapy is a promising approach to increase the survival rate and minimize the morbidity from current HNSCC treatments, all while reducing toxicity to patients. Single target drug therapies do not suffice to completely inhibit signaling pathways necessary for tumor survival. The purpose of this study was to investigate the effect on the proteome of shutting down two RTKs on HNSCC survival. The data suggests that treatment with the combination of EGFR and IGF1R inhibitors has a significant combination effect on cytotoxicity, thus improving the efficacy of the individual drugs. We found that the combined treatment with EGFR and IGF1R inhibitors led to further inhibition of proteins that are affected by the single drugs, which we define as a potentiative effect. We did not observe unique epitopes emerge from the drug combination. Interestingly, our PCA analysis indicated cell line specific effects on the proteome, with both common and unique loadings across the cell lines. Analysis of the cell line genomes from the CCLE illustrated the genetic differences between cell lines.[11] Therefore, HNSCC tumor heterogeneity must be understood and prioritized when developing effective targeted therapies.

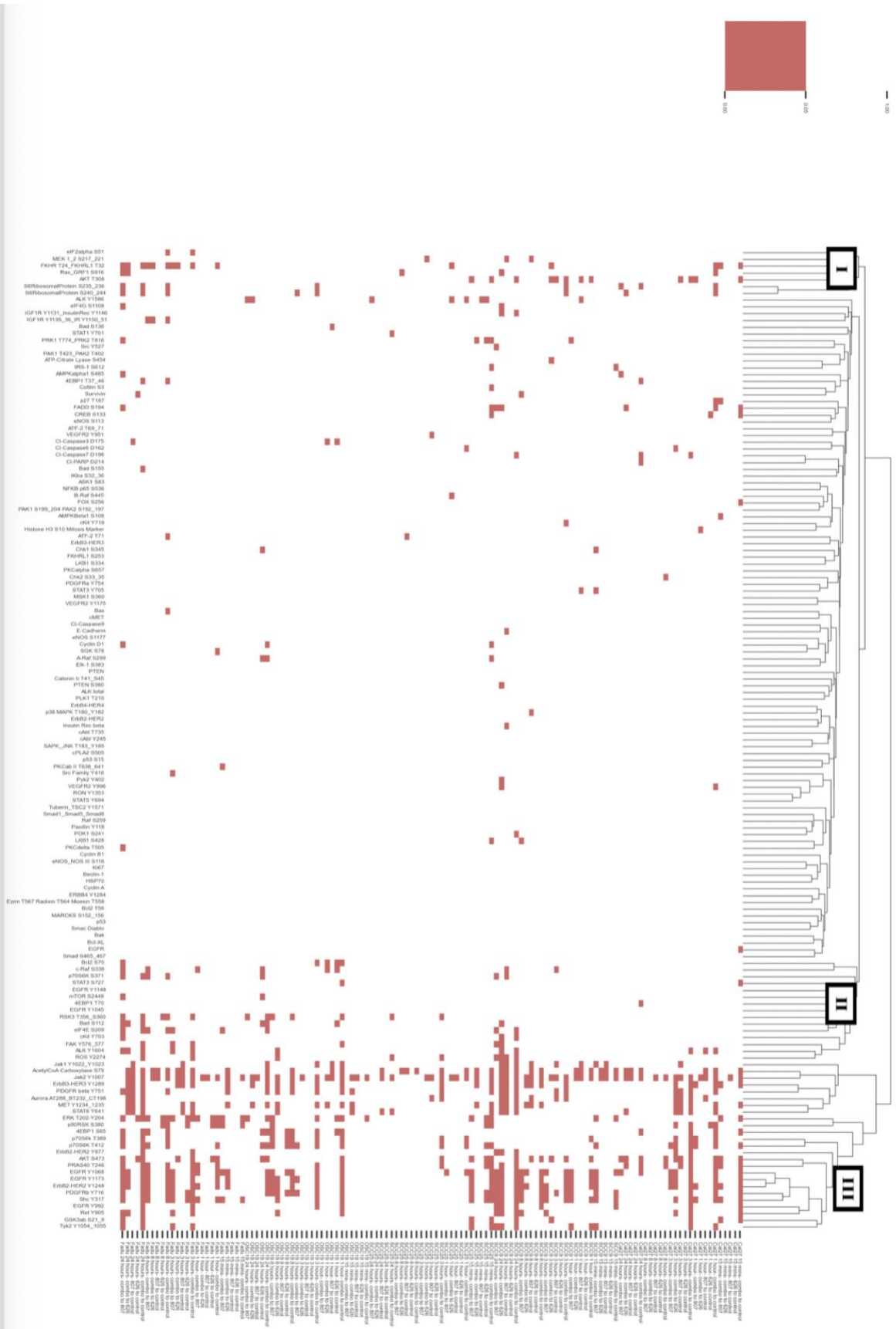

Figure 2: T-test Results. Comparisons in red are statistically significant with a significance level of 0.05 used. Comparisons between conditions are on the x axis. Epitopes are on the y axis. Three clusters were identified.

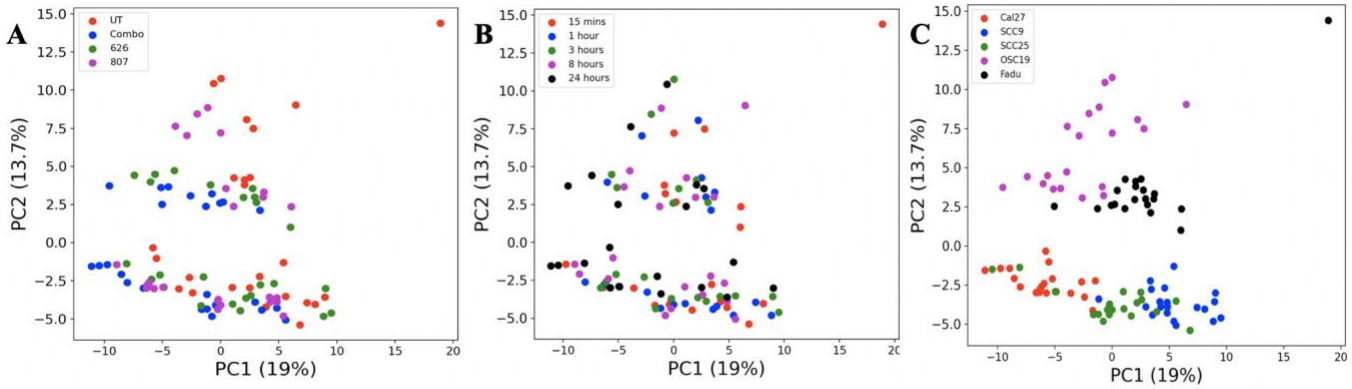

Figure 3: Principal Component Analysis Plots. PCA plots were generated in Python using two principal components. The data was colored by **A)** treatment, **B)** time point, and **C)** cell line. The axes represent the principal components and their percent variances.

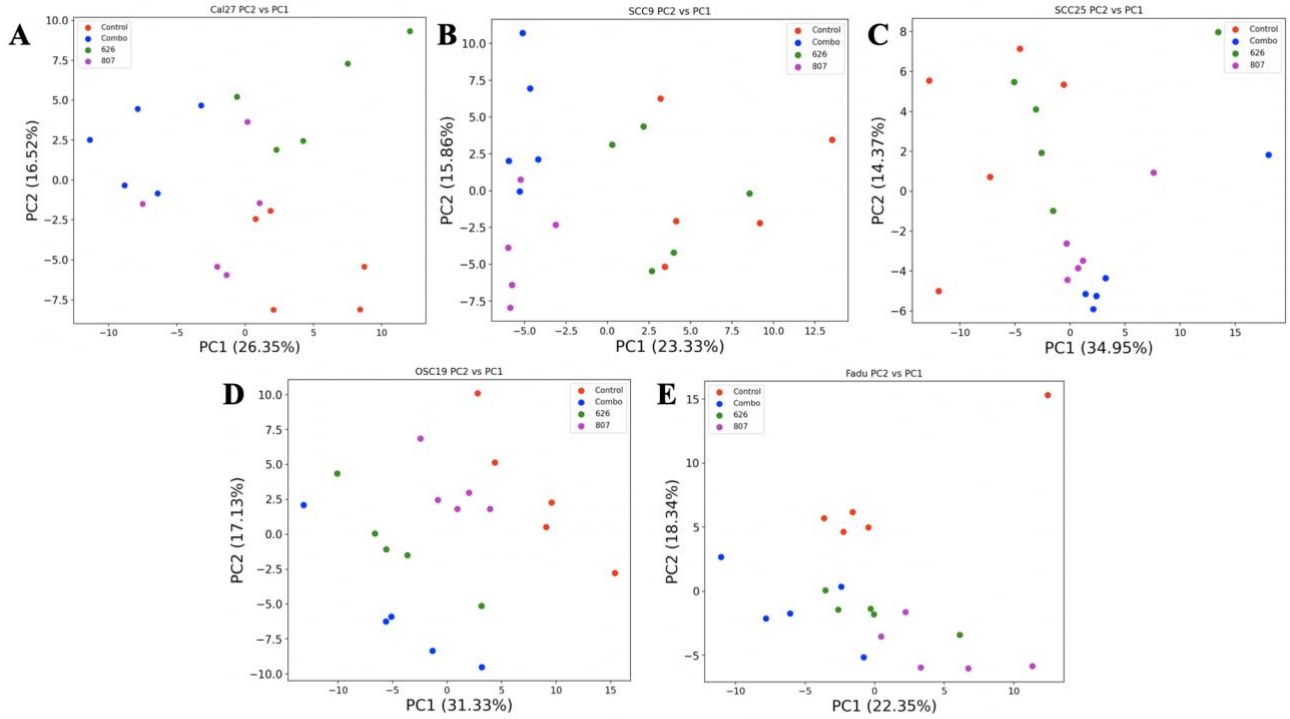

Figure 4: Cell Line Principal Component Analysis Plots. PCA plots were generated for each cell line. Principal components are on each axis with corresponding percent variances. The data for each cell line was color-coded based on treatment (control, BMS599626, BMS754807, and combination). **A)** Cal27 plot, **B)** SCC9 plot, **C)** SCC25 plot, **D)** OSC19 plot, and **E)** Fadu plot.

Future experiments will be performed in order to determine how the two receptors interact. Prior research suggests that EGFR and IGF1R communicate with matrix metalloproteinases (MMPs) in the cell membrane as a mechanism for resistance. Western blots looking at phosphorylation sites of EGFR and IGF1R after treatment with MMP inhibitors will generate evidence to support or dispute this hypothesis.

We acknowledge that RPPA experiments have limitations and antibody staining is not fully reliable. Additionally, the RPPA data contained holes in which no data for that epitope/condition was collected. Since there were replicates, trials were averaged in order to work around missing data.

Using a combinatorial treatment is a much safer alternative to current therapeutic options, and reduces the risk of relapsing because resistance mechanisms are being targeted. Ultimately, this drug combination could increase HNSCC patient survival in the long-term.

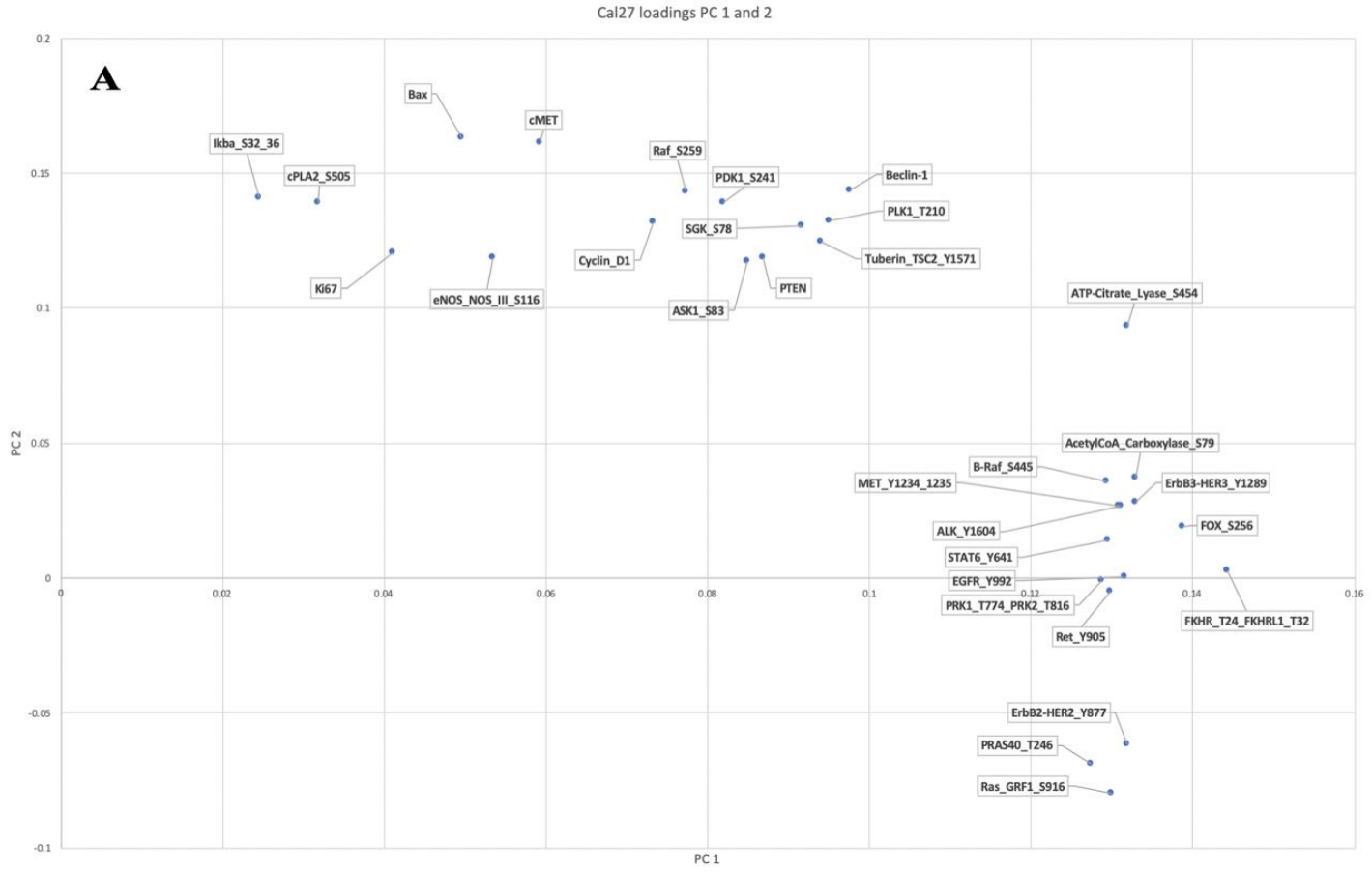
Cal27 loadings PC 1 and 2
A
Bax
cMET
Ikba_S32_36
Raf_S259
cPLA2_S505
PDK1_S241
Beclin-1
PLK1_T210
SGK_S78
Cyclin_D1
Tuberin_TSC2_Y1571
KI67
eNOS_NOS_III_S116
PTEN
ASK1_S83
ATP-Citrate_Lyase_S454
AcetylCoA_Carboxylase_S79
B-Raf_S445
MET_Y1234_1235
ErbB3-HER3_Y1289
ALK_Y1604
FOX_S256
STAT6_Y641
EGFR_Y992
PRK1_T774_PRK2_T816
FKHR_T24_FKHRL1_T32
Ret_Y905
ErbB2-HER2_Y877
PRAS40_T246
Ras_GRF1_S916
PC 1
PC 2

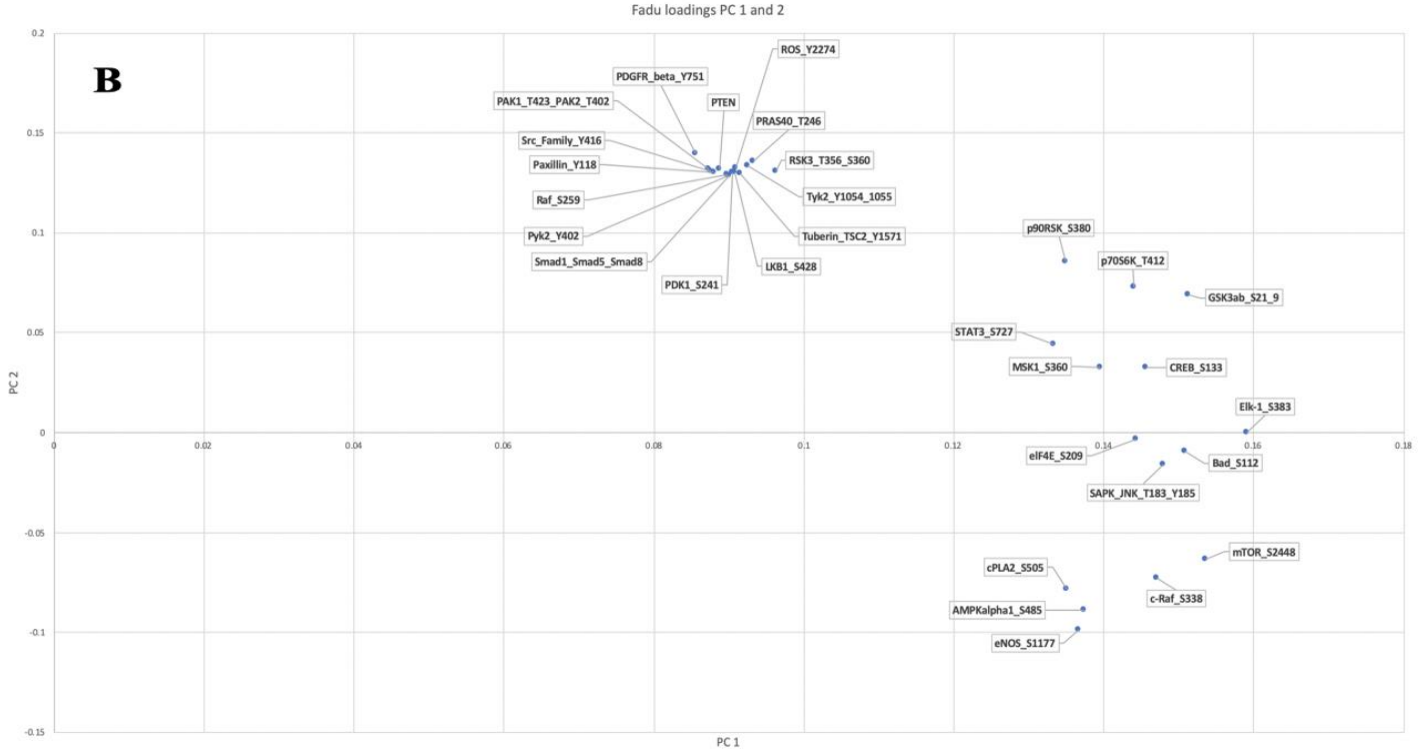
Fadu loadings PC 1 and 2
B
ROS_Y2274
PDGFR_beta_Y751
PAK1_T423_PAK2_T402
PTEN
PRAS40_T246
Src_Family_Y416
RSK3_T356_S360
Paxillin_Y118
Raf_S259
Tyk2_Y1054_1055
Pyk2_Y402
Tuberin_TSC2_Y1571
Smad1_Smad5_Smad8
LKB1_S428
PDK1_S241
p90RSK_S380
p70S6K_T412
GSK3ab_S21_9
STAT3_S727
MSK1_S360
CREB_S133
Elk-1_S383
eIF4E_S209
Bad_S112
SAPK_JNK_T183_Y185
mTOR_S2448
cPLA2_S505
c-Raf_S338
AMPKalpha1_S485
eNOS_S1177
PC 1
PC 2

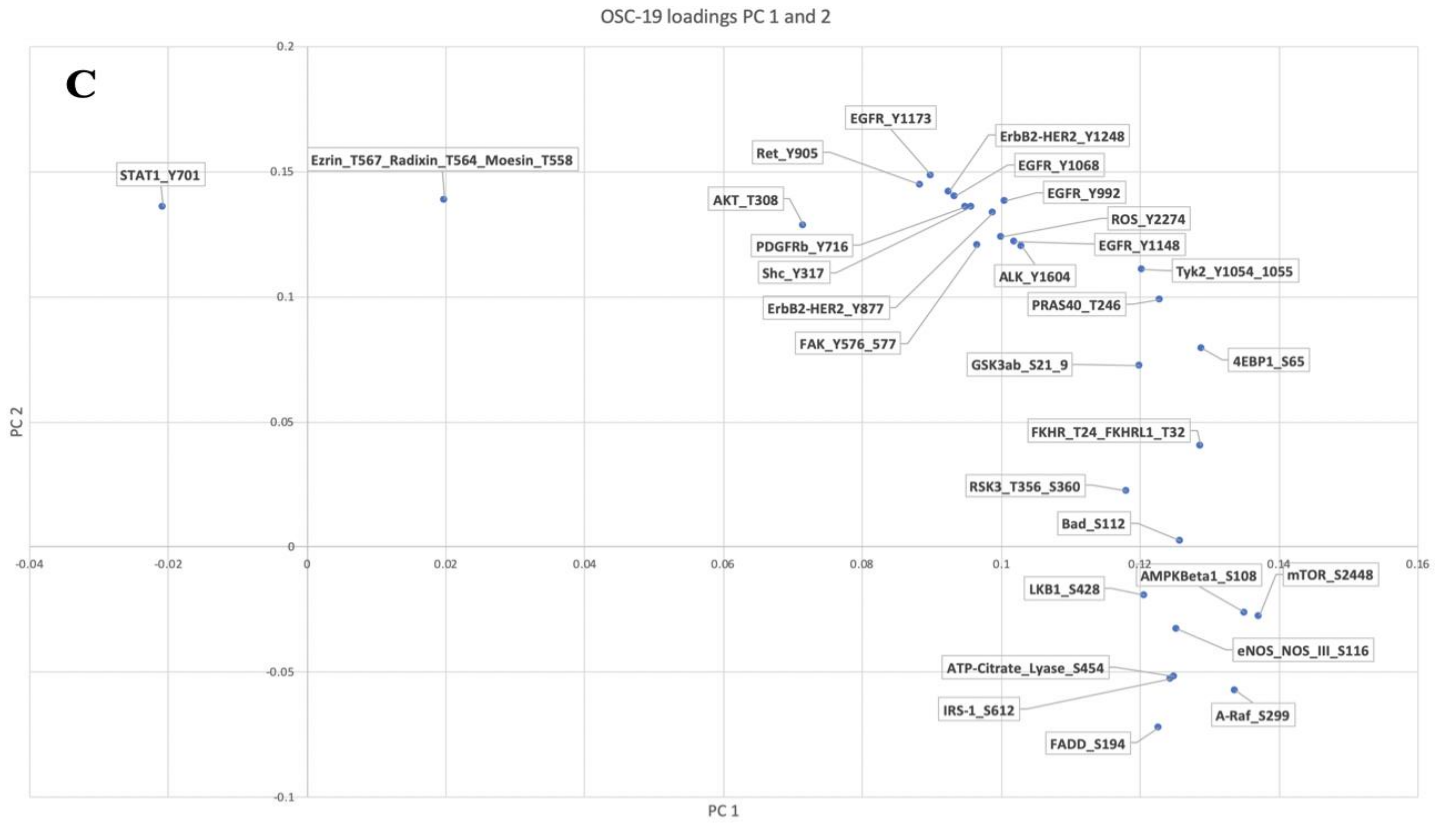
OSC-19 loadings PC 1 and 2
C
EGFR_Y1173
ErbB2-HER2_Y1248
Ret_Y905
Ezrin_T567_Radixin_T564_Moesin_T558
STAT1_Y701
EGFR_Y1068
EGFR_Y992
AKT_T308
ROS_Y2274
PDGFRb_Y716
EGFR_Y1148
Shc_Y317
ALK_Y1604
Tyk2_Y1054_1055
ErbB2-HER2_Y877
PRAS40_T246
FAK_Y576_577
GSK3ab_S21_9
4EBP1_S65
FKHR_T24_FKHRL1_T32
RSK3_T356_S360
Bad_S112
AMPKBeta1_S108
mTOR_S2448
LKB1_S428
eNOS_NOS_III_S116
ATP-Citrate_Lyase_S454
IRS-1_S612
A-Raf_S299
FADD_S194
PC 2
PC 1

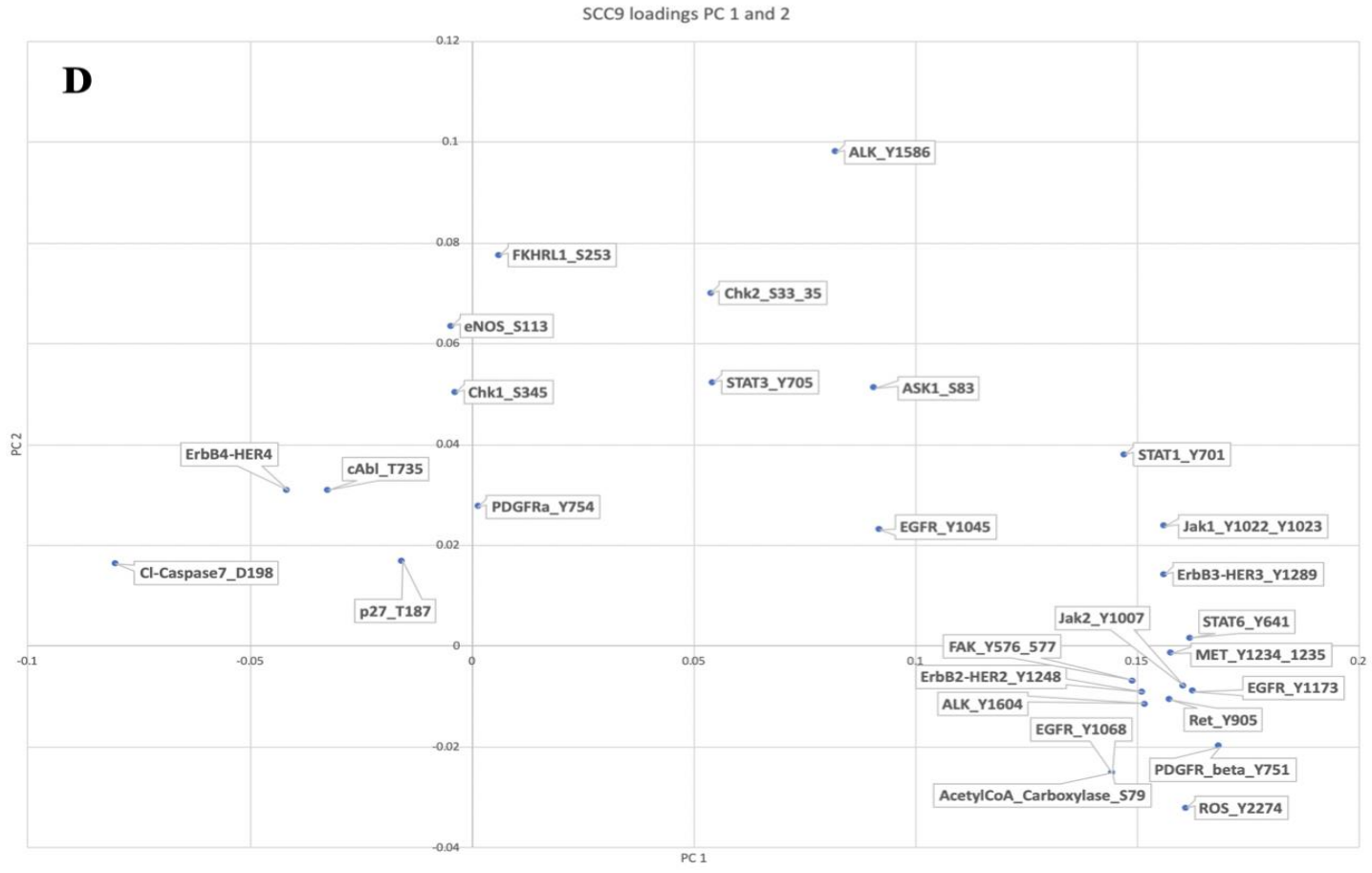
SCC9 loadings PC 1 and 2
D
ALK_Y1586
FKHRL1_S253
Chk2_S33_35
eNOS_S113
Chk1_S345
STAT3_Y705
ASK1_S83
ErbB4-HER4
cAbl_T735
STAT1_Y701
PDGFRa_Y754
EGFR_Y1045
Jak1_Y1022_Y1023
Cl-Caspase7_D198
ErbB3-HER3_Y1289
p27_T187
Jak2_Y1007
STAT6_Y641
FAK_Y576_577
MET_Y1234_1235
ErbB2-HER2_Y1248
EGFR_Y1173
ALK_Y1604
Ret_Y905
EGFR_Y1068
PDGFR_beta_Y751
AcetylCoA_Carboxylase_S79
ROS_Y2274
PC 2
PC 1

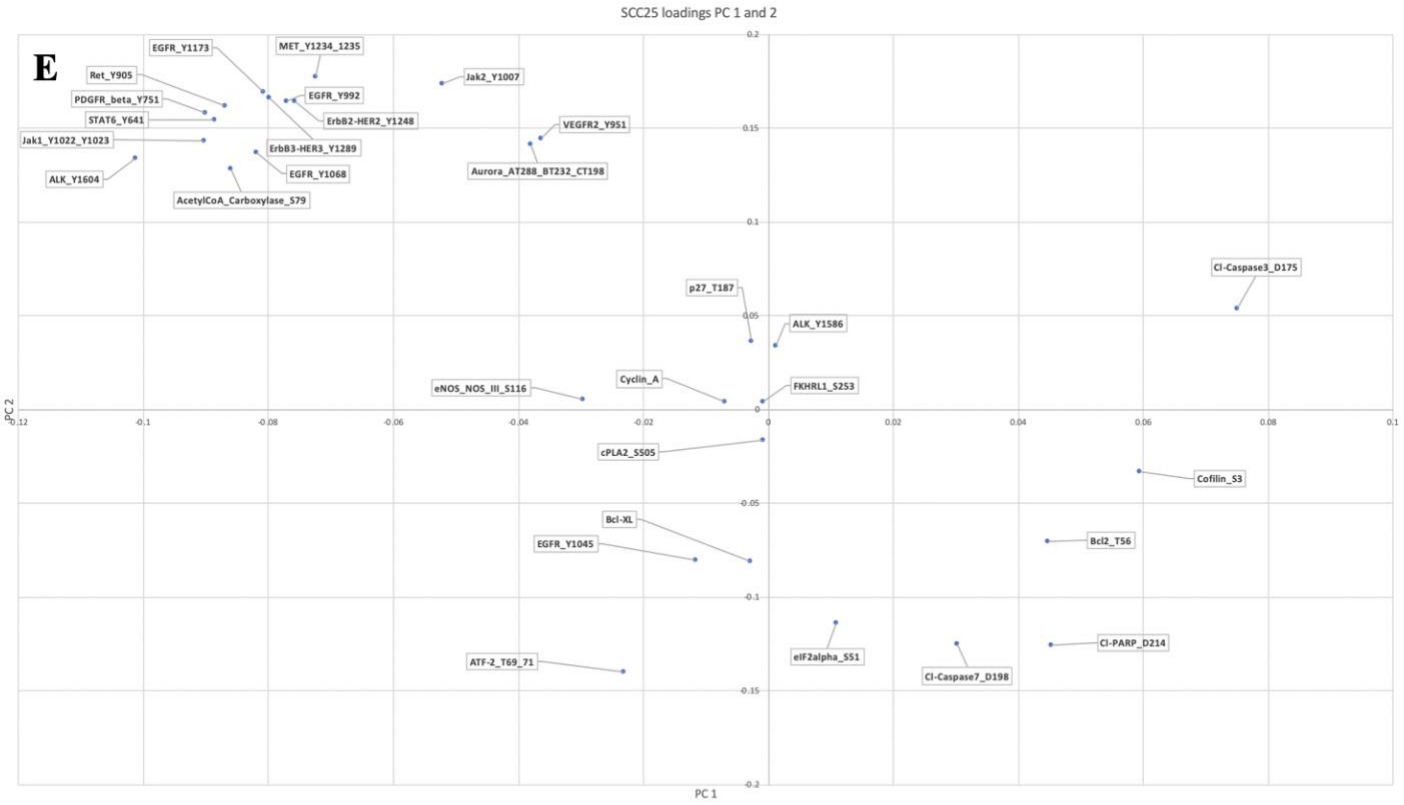

Figure 5: Cell Line PCA Loadings. Loadings for each epitope were calculated in Python and ranked. Top 15 epitopes with largest loadings for each principal component were plotted. Greater distance from the origin signifies greater impact on variance. Loadings plots for **A)** Cal27, **B)** Fadu, **C)** OSC-19, **D)** SCC9, and **E)** SCC25.

Materials and Methods

Log FC

The RPPA data contained three trials per condition, so the trials were first averaged to obtain a single value for each epitope. To calculate log fold changes, log base 2 of the data was used, with the treatment being divided by the control and subtracting by 1. To generate heatmaps with and without clustered axes in Python, the *seaborn* package was used along with *matplotlib, pandas, and numpy.* To create the compressed heatmaps, conditions from the same time point/cell line were averaged and no new Python packages were utilized.

T-tests

For unpaired t-tests, we used the packages *numpy, math, pandas,* and *scipy.*stats, and to generate FDR adjusted p values, the package *statsmodels.stats.*api was used. The same packages as those used to create the log FC heatmaps were used to plot the p-values.

PCA and loadings

In Python, *numpy, matplotlib, sklearn.decomposition,* and *sklearn.preprocessing* packages were used to generate principal components and all plots. Three components were of interest since these accounted for >50% of the variance in the data. Averaged raw data from Excel was utilized. When plotting cell line PCAs, the same data was used for only one cell line at a time. The PCA and loadings functions from *sklearn.decomposition* were used to calculate loadings for each epitope. In Excel, these values were ranked to find the top 15 epitopes in each principal component and loadings plots were generated.

Gene Mutations

Similarities between the list of gene mutations from cBioPortal and the lists of each cell line's mutations were determined in Excel. Proteins appearing on both lists were given a value of 1 while all others were given a value of 0. This table of 1s and 0s was uploaded to Python and proteins with a value of 1 were displayed in red. Plotting methods mentioned previously were used.

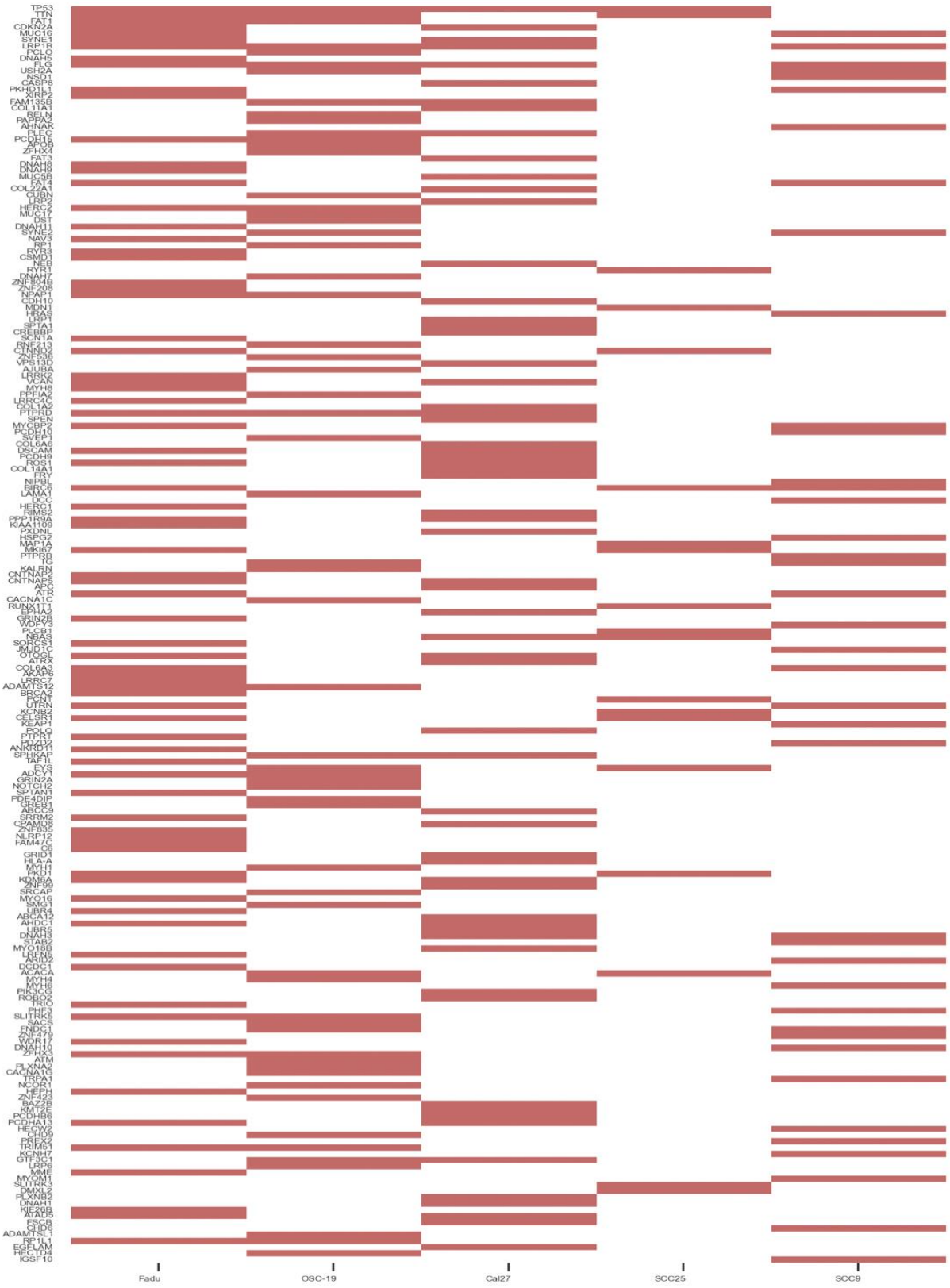

Figure 6: Cell Line Gene Mutations. Cell lines are on the x axis and gene mutations are on the y axis. Red signifies mutated epitopes that the cell line has in common with 515 HNSCC patient samples from cBioPortal.

End Matter

Author Contributions and Notes

S.H. D.G., and M.J. designed research, S.H. performed research, and S.H. wrote the paper. D.G. edited the paper. The authors declare no conflict of interest.

Acknowledgments

I would like to thank Dr. Daniel Gioeli and Dr. Mark Jameson for their advising throughout the project as well as the members of the Gioeli and Jameson laboratories for helpful discussions. I would also like to thank Dr. Shannon Barker and other BME faculty for their support.

References

1. Pulte, Dianne, and Hermann Brenner. "Changes in survival in head and neck cancers in the late 20th and early 21st century: a period analysis." *The oncologist* vol. 15,9 (2010): 994-1001. doi:10.1634/theoncologist.2009-0289
2. Vigneswaran, Nadarajah, and Michelle D Williams. "Epidemiologic Trends in Head and Neck Cancer and Aids in Diagnosis." *Oral and Maxillofacial Surgery Clinics of North America*, U.S. National Library of Medicine, May 2014.
3. Argiris, Athanassios, et al. "Head and Neck Cancer." *The Lancet*, vol. 371, no. 9625, 2008, pp. 1695–1709., doi:10.1016/s0140-6736(08)60728-x.
4. Cognetti, David M, et al. "Head and Neck Cancer: an Evolving Treatment Paradigm."*Cancer*, U.S.NationalLibraryofMedicine,1Oct.2008.
5. Hutcheson, Katherine A., et al. "Late Dysphagia after Radiotherapy-Based Treatment of Head and Neck Cancer." *American Cancer Society Journals*, John Wiley & Sons, Ltd, 17 May 2012.
6. Berns, Katrien, and René Bernards. "Understanding Resistance to Targeted Cancer Drugs through Loss of Function Genetic Screens." *Drug Resistance Updates*, Churchill Livingstone, 8 Nov. 2012.
7. Manchado, E., Weissmueller, S., Morris, J. *et al.* A combinatorial strategy for treating KRAS-mutant lung cancer. *Nature* 534**,** 647–651 (2016).
8. Roskoski, Robert. "The ErbB/HER Family of Protein-Tyrosine Kinases and Cancer." *Pharmacological Research*, vol. 79, 2014, pp. 34–74., doi:10.1016/j.phrs.2013.11.002.
9. Jameson, M. J., et al. "Activation of the Insulin-like Growth Factor-1 Receptor Induces Resistance to Epidermal Growth Factor Receptor Antagonism in Head and Neck Squamous Carcinoma Cells." *Molecular Cancer Therapeutics*, vol. 10, no. 11, 2011, pp. 2124–2134., doi:10.1158/1535-7163.mct-11-0294.
10. Weg M. Ongkeko, MD, PhD, Xabier Altuna, MD, Robert A. Weisman, MD, Jessica Wang-Rodriguez, MD, Expression of Protein Tyrosine Kinases in Head and Neck Squamous Cell Carcinomas, ***American Journal of Clinical Pathology***, Volume 124, Issue 1, July 2005, Pages 71-76, https://doi.org/10.1309/BTLN5WTMJ3PCNRRC
11. *Broad Institute Cancer Cell Line Encyclopedia (CCLE)*, portals.broadinstitute.org/ccle.

Supplemental Material

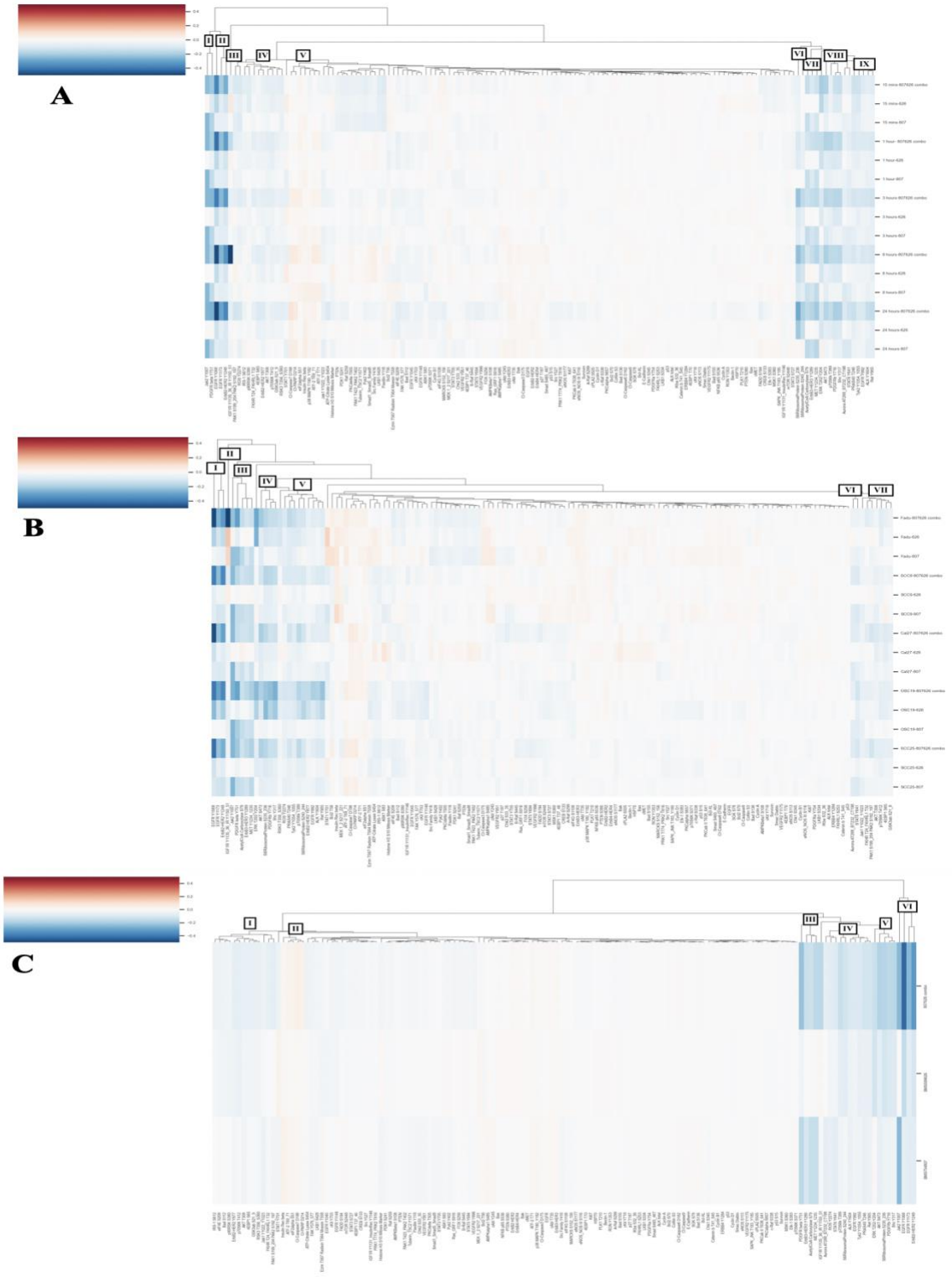

Supplemental Figure 1: Compressed Log FC Heatmaps. Data for each time point and/or cell line was averaged and plotted in Python. **A)** Compressed cell lines heatmap with epitopes on the x axis and drug treatment at each time point on the y axis. **B)** Compressed time points heatmap with epitopes on the x axis and drug treatment for each cell line on the y axis. **C)** Compressed cell lines and time points heatmap with epitopes on the x axis and drug treatment on the y axis.